Indian J. Met. Hydrol. Geophys. (1977), 28, 4, 447-458

551·576·4 : 551·507·362·2 : 551·521

Derivation of cloud top heights using HRIR data

N. S. BHASKARA RAO and V. P. SAXENA

Meteorological Office, Pune

(*Received 24 July 1974*)

ABSTRACT . Grid point temperatures derived from Radiance measurements of High Resolution Infra-Red sensors of Nimbus III were obtained from World Data Centre, Goddard Space Flight Centre, U.S.A. for specific areas on two selected days—7 Nov 1969 and 24 Jul 1969. The former is a day on which a severe cyclonic storm crossed the east coast of India near 17°N and the latter is a day on which monsoon was active generally over the country. The thermal fields were analysed and the cloud top heights derived in different sectors of the disturbed areas. The results have been discussed in terms of the synoptic situations and aerological data of nearby ground stations.

1. Introduction

1.1. The infra-red radiance data of scanning radio-meters on board the meteorological satellites have been utilised for various studies of the earth-atmospheric system. Of particular interest to operational problems is the High Resolution Infrared (HRIR) data, due to the fact that they provide information on the cloud distribution during night time and the radiance data is convertible to the surface temperature data of the field scanned. From the temperature data the three dimensional topography of the cloud fields can be obtained.

1.2. Warneck *et al.* (1967) have utilised the HRIR data from Nimbus II to map out the sea surface temperatures. Of particular interest in their investigation was the usefulness of these data in the detection of major ocean currents like the Gulf stream etc and shifts in their positions from time to time. The standard error between satellite data temperatures and those obtained from low flying aircraft was reported to be 2.3°K in 288 pairs of concurrent data.

1.3. The estimation of cloud heights from HRIR data is based on the principle that thick clouds radiate energy nearly like a black body, and the energy spectrum of the outgoing radiation corresponds to the temperature of the cloud top. It is reported* that in U.S.S.R, the operational units of the Weather Service receive surface temperature charts and maps of upper limits of clouds based on measurements of radiation temperatures in the 8-12μM wave band received from Kosmos satellites.

1.4. As yet the HRIR data have not been brought to operational use for obtaining cloud top heights in India. To the best of the knowledge of the present authors, no investigational work has so far been published on this subject from studies in the Indian area.

1.5. As heights of cloud tops are of considerable operational importance especially in aviation meteorology, this present study has been undertaken. It is also highly interesting to obtain an idea of the three dimensional structure of the cloud field associated with tropical cyclones during the transition months and of the monsoon cloud systems of the northern summer.

1.6. With a view to make a sample study of the types of cloud fields mentioned above, HRIR data for the required area for 7 November 1969 (a cyclonic storm case) and 24 July 1969 (a Monsoon clouding case) were obtained from the World Data Centre, Goddard Space Flight Centre, Maryland, U.S.A. The data are grid point temperature values. The data were analysed and the results are presented in this paper.

2. Data

2.1. The above data are from the radiance measurements made by the Nimbus III satellite. The resolution of the HRIR data is about 8 km at the sub-satellite point and deteriorates to about 35 km towards the east-west ends of the scans. The data for 7 November 1969 were from the night time scan (near about 1800 GMT over the required area). The data were requisitioned and were supplied for grid meshes of lengths 0.125, 0.250 and 0.625 of degrees (Lat./Long.). The area covered was from 10°N to 30°N and from 75°E to 85°E.

*WMO Executive Committee-XXII Scientific discussions— "Progress in the use of data from Satellites in the Hydro Meteorological Service of the USSR" Oct 1970

2.2. The data for 24 July 1969 was for the grid mesh of 0.125° and covers the area between 0° and 20° N and 70° to 80°E. Time of observation is around 1800 GMT.

2.3. Apart from the grid point data, the pictorial form of the cloud imagery for the entire scan from pole to pole were also supplied. In both the cases the required areas lie in the central regions of the scans and so the resolution of the sensor data is satisfactory.

3. Case I—Cyclonic Storm of 7 November 1969

3.1. *A brief history of the storm and synoptic conditions.*

3.1.1. A low pressure area moved into north Andaman Sea on 2 November 1969 which concentrated into a depression by 4th. Moving in westnorthwesterly direction it became a cyclonic storm on 5th and intensified into a severe cyclonic storm on 6th morning with its centre near Lat. 14°N, Long. 87°E. It continued to move in a westnorthwesterly direction and struck the Andhra coast near 17°N and lay with its centre at 1200 GMT on that day near Nidadavolu (about 17°N, 81.5°E). At 1800 GMT (the time of satellite data) its centre was near 17°N, 80°E. It weakened into a cyclonic storm during the night and next morning it lay with its centre near Hyderabad. It weakened further on 8th and moving in a northwesterly direction lay as a depression near Ahmednagar on 9th morning. The lowest pressure recorded was at Nidadavolu being 975.2 mb at 1730 IST of 7th and the corresponding pressure defect was 35.8 mb. The storm caused heavy flooding in the coastal districts of Andhra Pradesh particularly in the east and west Godavari districts causing damage to standing crops and loss of life.

3.1.2. The section of the cloud imagery pertaining to the storm area from orbit No. 2781 of Nimbus III is shown in Fig. 1. It can be seen from the picture that though the storm had crossed coast and advanced well inland, the cloud structure remains the features of a well developed storm out at sea with a central overcast mass and an outer structure of spiral bands. A secondary bright overcast area is seen just to the northwest of the central overcast mass of the storm.

3.1.3. Fig. 2 shows the surface isobaric system at 18 GMT with the cloud imagery in the background. The track of the storm and the rainfall recorded at 0830 IST on 8th are also shown in the figure. Five closed isobars drawn at 2 mb interval cover the storm area, the value of the lowest isobar being 1000 mb. The storm has apparently weakened considerably between 12 and 18 GMT of 7th.

Fig. 1. Cloud imagery of the storm obtained from HRIR sensors of Nimbus III Orbit No. 2781 on 7 Nov 1969. Approx. time 1800 GMT (Areas marked ABCD—please refer Fig. 7)

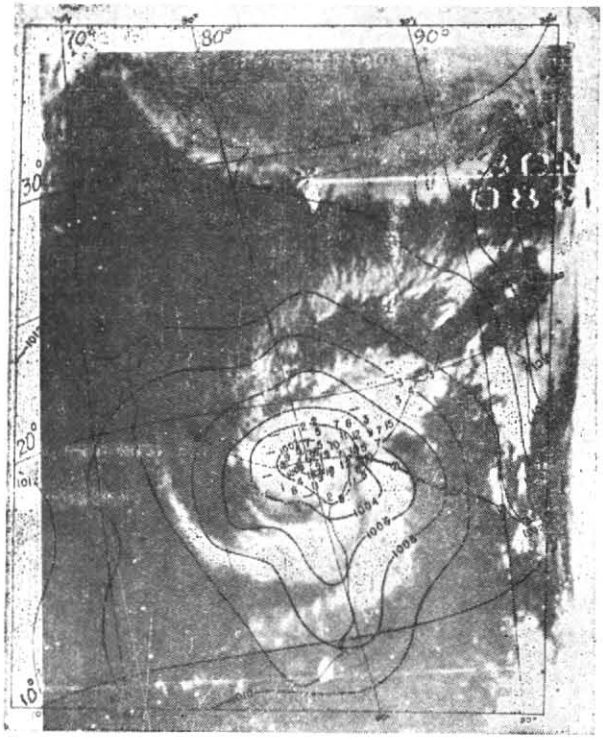

Fig. 2. Surface isobars at 1800 GMT on 7 Nov 1969 with cloud imagery in the background. The track of the storm and the rainfall amount recorded at 0300 GMT of 8 Nov 69 are a'so shown

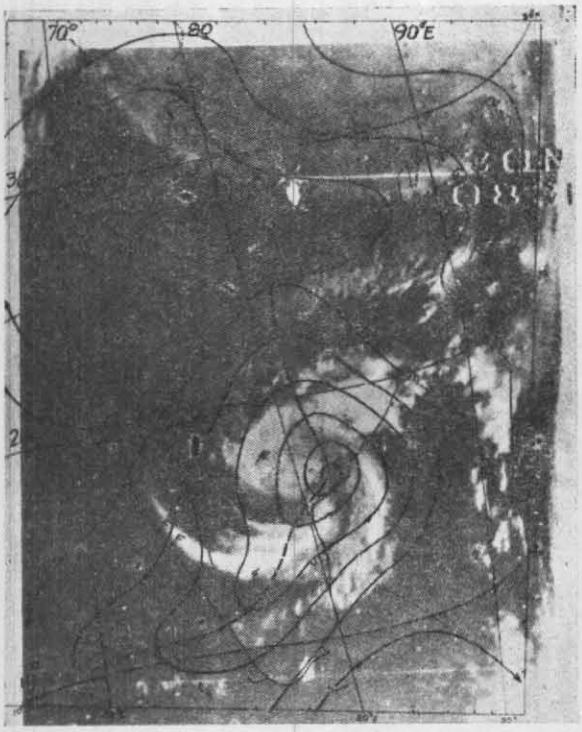

Fig. 3(a). 500 mb streamlines at 1200 GMT on 7 Nov 1969

Fig. 3(b). 200 mb streamlines at 1200 GMT on 7 Nov 1969

3.1.4. It may be mentioned here that there is a difference in the positions of the centre of storm as obtained from the cloud imagery and as seen from conventional data. The isobaric field had to be shifted by about 1° to the north and 1° to the west so that the centre of the storm obtained by the above two methods coincide. This may partly be due to the tilt of the system with height as the storm was weakening and the satellite pictures tend to reflect the upper portions of the storm.

3.1.5. The shift also makes the rainfall pattern more comparable with the brightness pattern seen in the satellite picture—for example the heavy rainfall amounts near 19° N along the east coast coincide with the bright overcast area to the northeast of the storm. It is stated in "Nimbus III User's Guide" that the grid points are electronically superimposed on the film and manually checked to maintain an accuracy of better than 1 degree (Lat./Long.) at the sub-satellite point. Srinivasan (1970) discussed the various types of errors which enter into operational gridding of APT pictures with particular reference to Indian area. Considering all the factors the correction given to the HRIR picture ocation appears to be reasonable.

3.1.6. The 500 mb and 200 mb streamline patterns are shown in Figs. 3(a) and 3(b) respectively with the cloud imagery as an underlay. In keeping with the shift given to the isobaric chart, the corresponding shift was also given to these upper air charts. In this case there is a time difference of 6 hours between the time of the upper charts and the time of the satellite picture. Hence the upper air systems lie about 1° (Lat./Long.) to the eastsoutheast of the corresponding cloud features. The well marked spiral band to the south (Fig. 3a) lies at its eastern and along the trough extending from the storm and the axis of the trough is shown by the thick dashed line. This kind of cyclonic wind shear was also seen at the lower levels. The other band seen on the satellite picture also seems to follow the general flow pattern. The anticyclonic system to the northwest of the storm over Rajasthan is characterised by clear skies.

3.1.7. The chief features seen on the 200 mb stream line chart are (*i*) strong diffluent field over the storm area, (*ii*) an anticyclonically curved flow which seems to agree with the curve of cirrus top of the spiral band to the south of the centre and (*iii*) strong westerly winds north of 25°N. The diffluent field and the possible divergence may

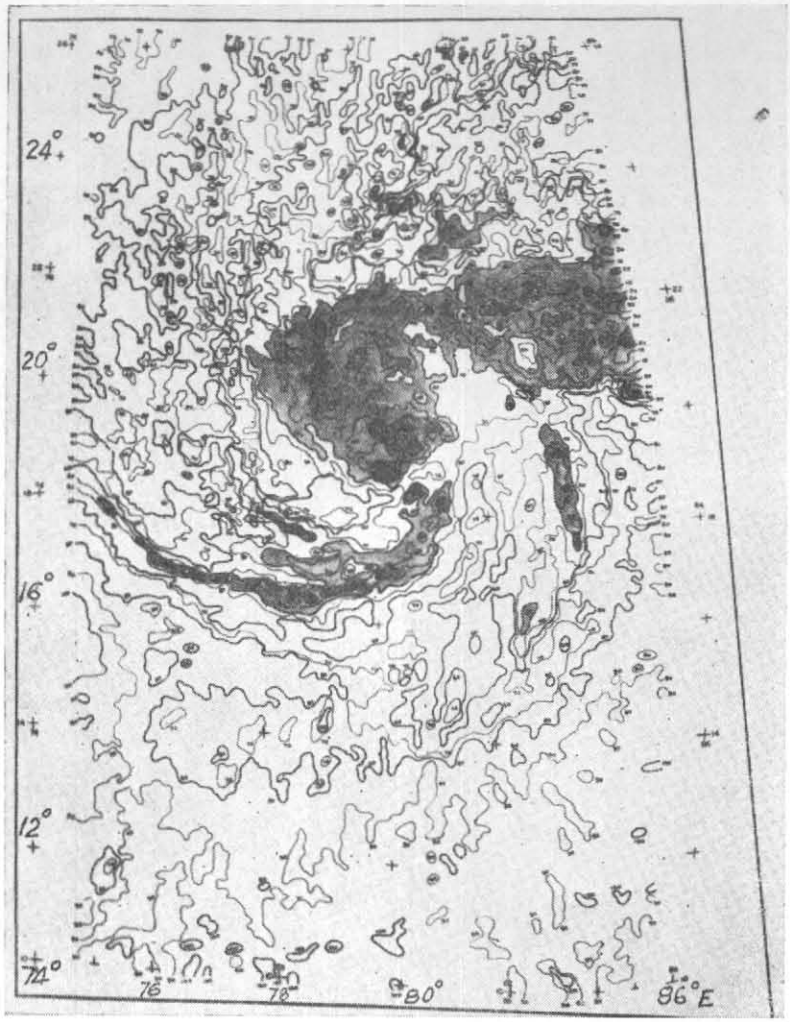

Fig. 4. Isothermal analysis of the temperature field obtained from Nimbus III HRIR data of 1800 GMT of 7 Nov 1969

be partly due to the strong convective activity in the area. Fujita (1968) has shown that large masses of convective clouds transport considerable amount of air from the lower to upper tropospheric levels, where they cause strong horizontal divergence. His studies were based on winds derived from ATS 1 and ATS 3 data.

3.2. *Satellite temperature data analysis*

3.2.1. The temperature data for the finest mesh (grid length 0.125°) have been plotted to scale of an enlargement of the cloud imagery shown in Fig. 1. The isothermal analysis of the plotted data is shown in Fig. 4. The complexity of the temperature field seen on the figure indicates that wide variations of the cloud top heights can occur over short distances. The analysis also indicates that no thick cirrus top exists over the disturbed area as rapid variations in the temperature data are also observed in the two heavy overcast areas with a few gaps of relatively much warmer temperatures in the overcast areas.

3.2.2. The extremes of temperatures found in the data are 200°K on the lower side and 300°K on the higher side. Very low temperatures (210°K or less) are observed in the central overcast area, in the spiral bands to the south and also in the heavy overcast area to northeast. Along the spiral band to the south also, pockets of such low temperatures are also seen.

3.3. *Sea surface temperature*

3.3.1. Areas of temperature above 300°K are found to lie both over land and sea. Over the sea areas they lie mostly to the south of 12°N indicat-

ing the sea surface temperature to be about 27° C. Braun(1971) discussed the limits of the accuracy of infra-red radiation measurements of sea-surface temperature from satellites and stated that the greatest accuracy with which the temperature can be determined using one or two channel radiometer working in the 3.4 to 4.2 μM spectral region is about 2 to 3°C.

3.3.2. A direct comparison of the highest temperatures in the apparently cloud free areas was made in the study. Fig. 5 shows the ships' observations in the Bay of Bengal from 5 to 8 November 1969. The sea surface temperature is around 29°C. The highest temperatures of 300°K from HRIR data agrees fairly well with ships' observations within the limits of the experimental errors.

3.4. *Heights of cloud tops*

3.4.1. The lowest temperatures apparently refer to the tops of the highest clouds in the area. However, according to "Nimbus III User's Guide" temperatures below 210°K may not be realistic. Even assuming that all temperatures below 210°K are truncated to 210°K, it shows that the maximum heights were around 13-14 km a.s.l.

3.4.2. To obtain the heights of cloud tops from the satellite temperature data, an average temperature-height profile was drawn taking the 1200 GMT data of 7th and 0000 GMT data of 8th from the stations lying in the affected area. It was noticed that the gradients of temperature in the area were not significantly large justifying the use of an average profile.

3.4.3. In Fig. 4, the areas whose temperatures were below 240°K have been shaded lightly and those below 220°K heavily. As can be seen the correspondence between the shaded areas and major features seen on the cloud picture (Fig. 1) is good. Clouds with tops at very great heights (12 km and above) were found in the central overcast mass, the bright cloud mass northeast of it and in the well marked band south of the storm centre.

3.4.4. Cross-sectional profiles of cloud-top heights through the storm centre are shown in Figs. 6 (a) and 6(b), the former profile being along 80°E meridian and the latter being along Lat. 17°N.

3.4.5. It can be seen from Fig. 6(a) that cloud tops of 9 km and above practically cover the section from about 16°N to about 22°N. Judging from the rainfall distribution which does not amount to much north of 19°N the high cloud tops between 19°N and 22°N may be mostly those of cirrus clouds with a few cumulus cells below and a few tall

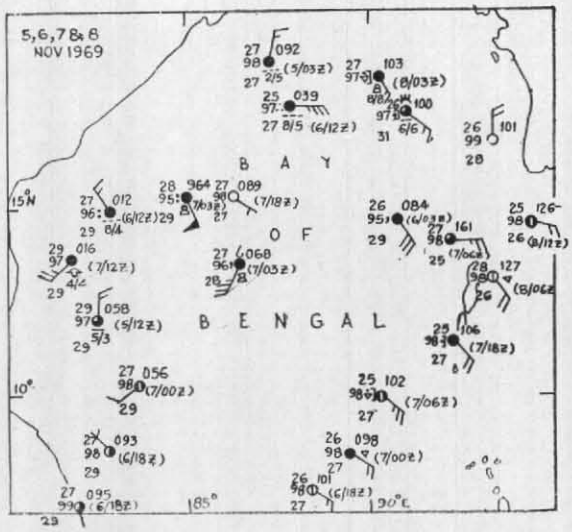

Fig. 5. Ships observations from the Bay of Bengal from 5 to 8 Nov 1969

clouds protruding above the cirrus layer. The very low heights indicated south of 13°N refer to equivalent surface temperatures and to some amount of low cloud development in that sector. Towards the northern end the cloud picture reveals practically clear skies. Hence the heights indicated may apparently refer to the surface temperature which in that area was around 20°C (giving equivalent height of 1.5 km a.s.l.). A few cumulus clouds of sizes below the resolution of the sensors may also have been present.

3.4.6. The zonal cross-section shown in Fig. 6(b) exhibits some typical characteristics of a cyclonic storm with the lowering of cloud tops near about the centre and wall-clouds around the centre extending in height to about 12km a.s.l. Hubert *et al.* (1969) got similar radial profiles for Hurricane *Inez* (for 4 Oct 1966). The difference in the longitudinal position of the central area based on conventional data and that shown by this cross-section is about a degree. The two secondary maxima in cloud top heights region on the flanks apparently refer to adjacent band structure of the storm.

3.5. *Cloud amount and distribution*

3.5.1. Krishna Rao (1970) discussed the estimation of cloud amount and heights from satellite I.R. data. A analysis was also made of the present data on similar lines. The grid point value data in different 1°-squares were taken and the percentage frequency distribution of temperatures falling in 10°C intervals were worked out. The histograms thus obtained for 4 sample 1° squares are shown in Fig. 7. Fig. 7(a) refers to the dense

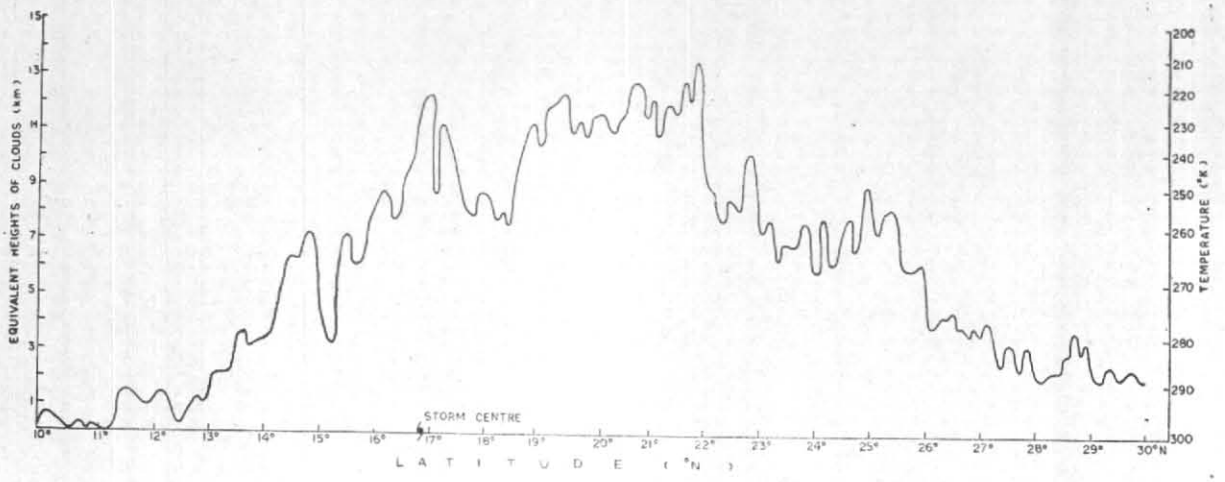

Fig. 6(a). Meridional profile of the temperature data along Long. 80°E obtained from the HRIR data of 7 Nov 1969.

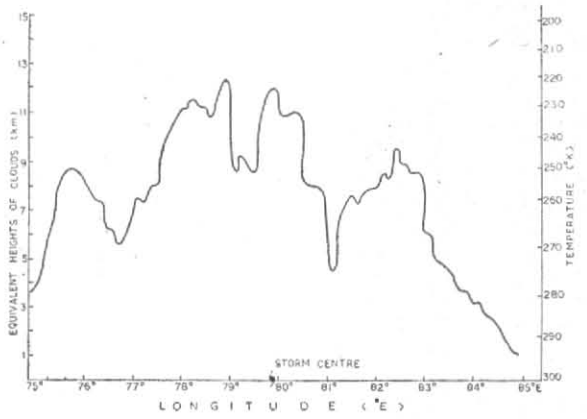

Fig. 6(b). Zonal profile of the temp data along Lat. 17°N obtained from the HRIR data of 7 Nov 1969

overcast mass to the northeast of the storm centre which is the brightest area in the whole picture (Fig. 1). It can be seen even in this area which appears almost uniformly bright in the cloud imagery that cloud tops are at the heights ranging from 4 to 14 km. In HRIR imagery the absence of shadows and highlights (which are found in TV picture data), makes the interpretation of night time imagery more difficult unless the actual temperature values are available. Nearly 50 per cent of the temperature value lie at or below 240°K showing that *Cb* tops with their *Ci* canopies occupy approximatey half the area. On the other hand temperatures as high as 280°K recorded in this area show that no dense cirrus covers the entire area. The conventional data indicated mainly low stratus cloud in the area with precipitation at 1800 GMT of 7 November 1969. Vizag reported *Cb* clouds. Rainfall recorded at 0300 GMT of 8 April 1969 (Fig. 2) indicated heavy falls in the area.

3.5.2. Fig. 7(b) refers to the central overcast mass. In this area about one-fourth of the data indicated temperatures below 240°K and the extreme values of 210°K were not found. The average height of the cloud tops works out to be about 9 km, the range being about 4-12 km. About 45 per cent of the data refer to cloud tops at or about 9 km. The conventional data indicated low stratus and thick altostratus. Heavy precipitation recorded on 8th in the area indicates heavy showers and convective activity.

3.5.3. Fig. 7(c) is chosen in the striated band to the north of the storm. This indicates large cumulus build-ups with cirrus outflow in this area. Fairly widespread large cumulus/*Cb* with tops around 6-9 km cover nearly 80 per cent of the area. Even though in the cloud imagery picture some areas appear free from clouds the highest temperatures of only 10°C are found in this region

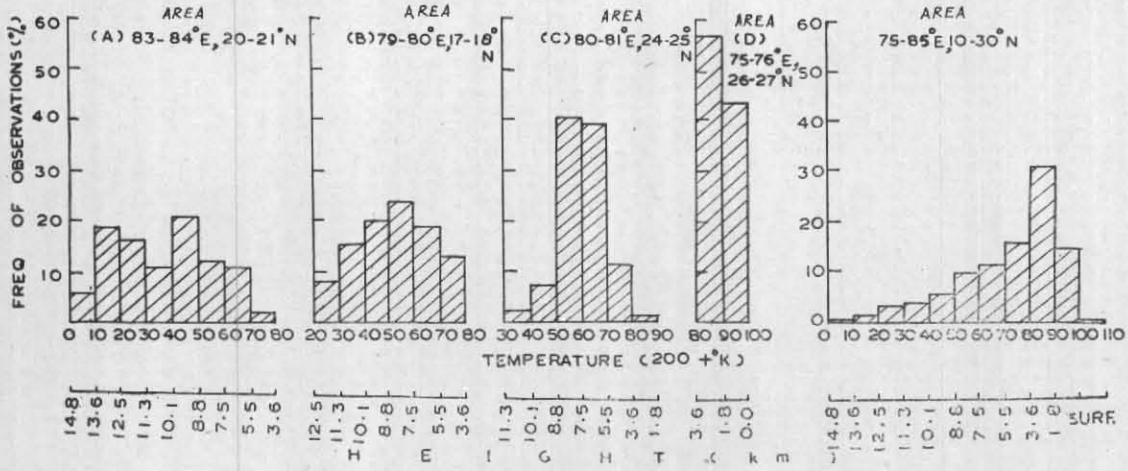

Fig. 7 Fig. 8

Fig. 7. Histograms showing the frequency distribution of temperature falling in 10°C intervals for 4 sample 1° squares in the storm area (7 Nov 1969). Equivalent heights are also given in the diagram. Area 'A' lies over the dense mass to the NE of centre overcast area. Area 'B' falls over the centre overcast area. Area 'C' falls over the striated cloud bands to the north of the storm and area 'D' to the darkest part to the NW of the storm (Areas shown in Fig. 1)

Fig. 8. Percentage frequency distribution of temperatures for the entire are a (75°–85°E, 10°–30° N). Equivalent heights are also shown.

which is atleast 10°lower than the actual temperatures as reported at 1800 GMT from the surface stations. This indicates that some scattered clouds of areal extent below the resolution of the instrument are present in the area. The 1800 GMT data in the area indicated mainly high clouds. Apparently the observations being made in night time, some of the smaller convective clouds might have been missed.

3.5.4. Fig. 7(d) is chosen in one of the darkest regions of the picture (Lat. 26°-27°N, Long. 75°-76°E). The temperature range found in this area is from 280° to 300°K. The surface temperatures reported from land station in this area were 27°C which agrees with the highest temperature 300° K obtained. The lower temperature show that some small scattered low clouds below the resolution of the sensors or scattered *Ci* cloud below the level of discernment are present in the area. Continental data indicate clear skies in this area.

3 5.5. Fig. 8 shows the percentage frequency distribution of temperatures for the entire area (75°-85°E, 10°-30°N). It is seen from this figure that cloud tops at 9 km and above occupy about 17 per cent of the area and cloud tops between 3 to 9 km occupy about 1/3 of the area. The remaining 50 per cent area is either free from clouds or occupied by scattered low clouds.

4. Case II — Southwest Monsoon clouding

4.1. *Synoptic situation*

For this study, 24 July 1969 was chosen, as on this day rainfall was nearly general in most parts of the country. The cloud imagery is shown in Fig. 9. The principal features of the clouds shown by the figure are (i) two long parallel bands of clouds one nearly along Lat. 6°N and another along Lats. 8°-10°N, (ii) other broken bands also lie parallel to Lats., and (iii) a very bright mass near 20°N, 80°E.

4.1.1. The 18 GMT surface chart of 24 July 1969 and the 12 GMT 850, 500 and 200 mb charts are shown in Figs. 10(a) to 10(d) respectively. The 24-hr rainfall chart of 03 GMT of 25th is also shown in Fig. 10(a). The chief features seen on the surface chart are (i) a well marked trough in the Comorin area; which is apparently associated with the marked convective activity seen in the satellite picture in those latitudes, (ii) a low pressure system over northeast Madhya Pradesh and adjoining Uttar Pradesh which lies in the general monsoon trough. The monsoon trough at its eastern end was dipping into west central and adjoining northwest Bay. The 850 mb chart shows that strong westerlies prevailed over the Peninsula and a well-marked cyclonic circulation over north Orissa. This was discernible at the 700 mb level also. At 500 mb level the east-west discontinuity runs

Fig. 9. Cloud imagery of the monsoon clouds over the Indian area and neighbourhood obtained from HRIR sensors of Nimbus III. Orbit No. 1360, 24 Jul 1969. Approximate time 1800 GMT (Areas marked EFGH please refer Fig. 11).

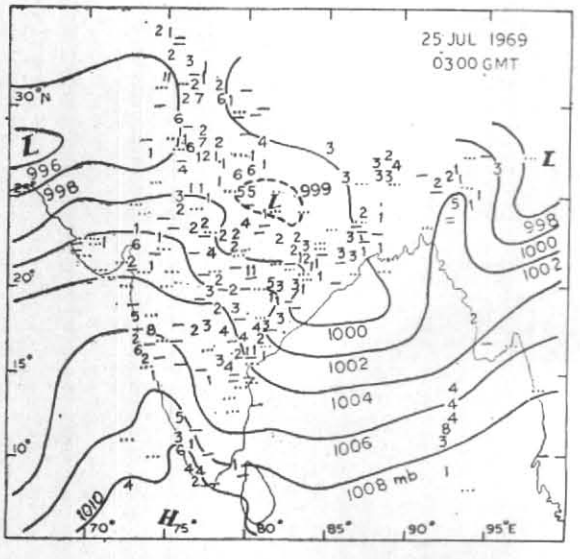

Fig. 10(a). Surface isobars at 1800 GMT on 24 Jul 1969 with the rainfall amounts at 0300 GMT of 25 Jul 1969 plotted.

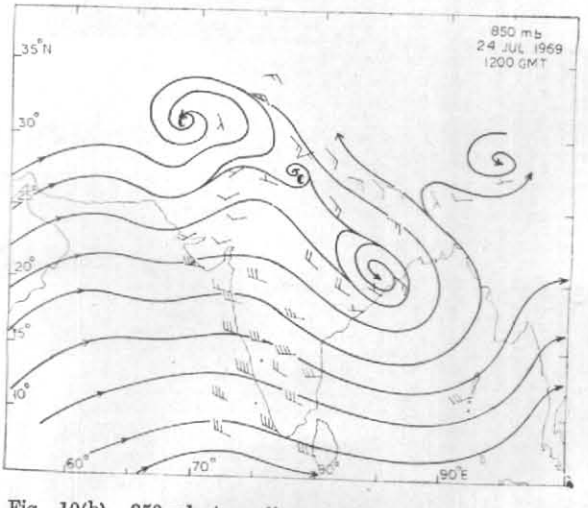

Fig. 10(b). 850 mb streamlines at 1200 GMT on 24 Jul 1969

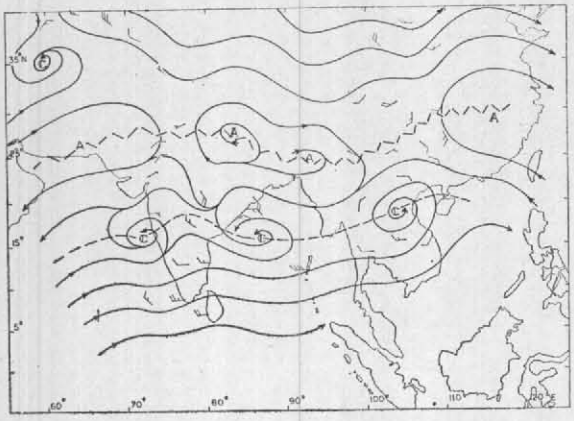

Fig. 10(c). 500 mb streamlines at 1200 GMT on 24 Jul 1969

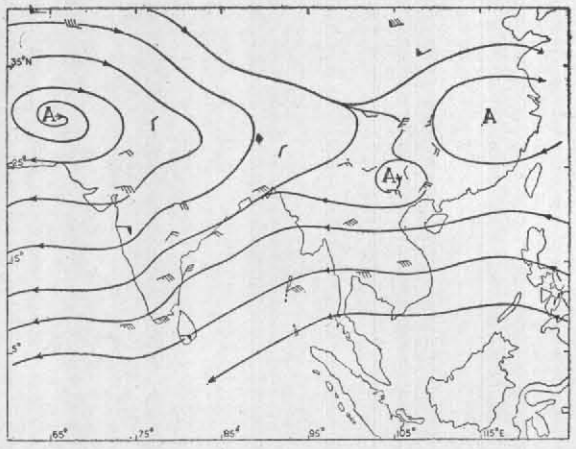

Fig. 10(d). 200 mb streamlines at 1200 GMT on 24 Jul 1969

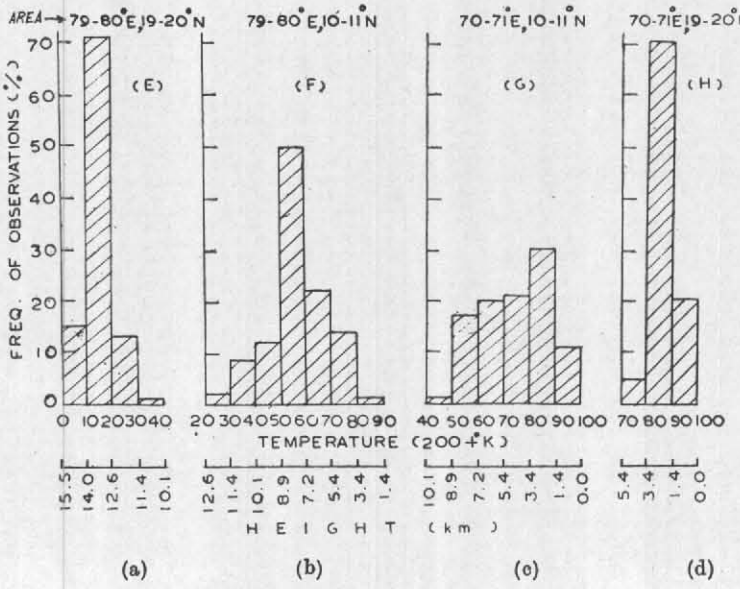

Fig. 11. Histograms showing the frequency distribution of temperatures falling in 10°C intervals for four sample 1° squares as shown in Fig. 9(Please see under section 4·2). Equivalent heights are also shown against the corresponding temperatures.

roughly along 17°N over Peninsular India. Easterlies of speeds 30-50 kt are seen at the 200 mb level over the Peninsula. The cirrus outflow from the parallel bands of clouds seen between 4° and 10°N is in keeping with the strong easterlies seen on this chart.

4·2 *Distribution of cloud amounts and heights*

4.2.1. As in the case of the cyclonic storm discussed in sections 3·4 and 3·5, the frequency distribution of the temperatures for 1° squares in different areas were calculated. Fig. 11 shows the histograms for four selected areas. Fig. 11 (area E on Fig. 9.) pertains to the brightest area seen on the picture. More than 86 per cent of the area refers to cloud tops at or above 12.5 km indicating that almost the entire area is covered by dense cirrus top of the *Cb* clouds. The rainfall figures also confirm good convective activity in the area covered by the overcast mass even though the rainfall reported from this particular 1° square is not much but thunderstorms were reported. There is no observation from this square on 18 GMT chart of 24 July 1969. However the nearby stations are heavily overcast with thick altostratus clouds being reported. The area received widespread rainfall on that day with isolated heavy falls being reported by nearby stations.

4.2.2. Area F (Fig. 11 b) refers to broken cloud region. Multilayered clouds with isolated *Cb* clouds covering about 20 percent area were

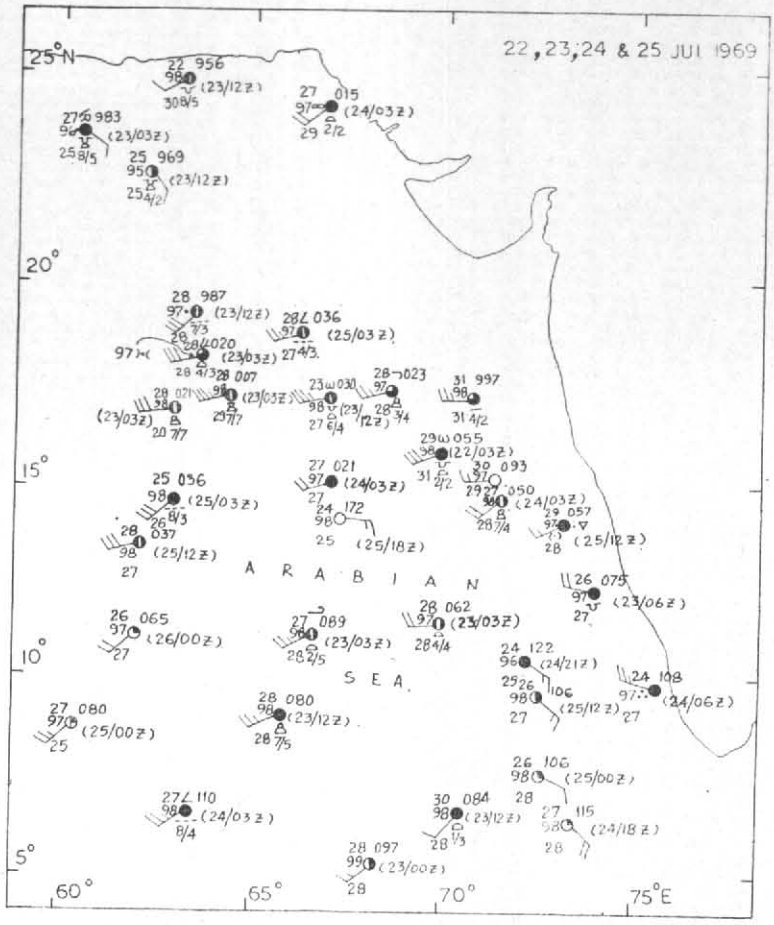

Fig. 12. Ships observations from the Arabian Sea from 22 to 25 July 1969

apparently present in this 1° square. The conventional data showed that the area was heavily overcast with low stratus and thick atlostratus beirg reported from all the stations in and around the area. Some scattered rainfall was recorded.

4.2.3. Area G (Fig.11 c) is chosen in a fairly dark region between two cloud bands. Broken low clouds with thin cirrus seem to be present as could be judged from the frequency distribution. The maximum temperature around 300°K apparently refers to sea surface temperature, indicating it to be about 27°C. Ships observations of the sea surface temperature from 22nd to 25th are shown in Fig. 12. Over the area concerned the temperatures seem to be around 27-°28°C which is in fair agreement. There is no conventional data in this area or nearby.

4.2.4. Area H (Fig.11d) is an other dark region. As compared to area 'G' this area appears to be more cloud free and is reflected in the frequency distribution of the temperatures. The presence of a sheet of a thin cloud below the level of discernment seems to be causing a general lowering of the temperature by about 15°C. There is no conventional data for this area also but nearby ships reported 2-3 okta of low cloud and some amount of medium clouds.

4·2·5. Fig. 13 shows the isothermal analysis of the plotted data between 4°-8°N and 70°-80°E with an enlargement of the cloud imagery system as an underlay. The noteworthy points seen on this figure are (*i*) the steep temperature gradients at the edges of the cloud bands and (*ii*) relatively slack temperature gradients over the overcast area, indicating that the major portion of the bright area is more or less at about the same temperature (same height), representative of *Ci* overcast, with a few small cells projecting above.

5. Some limitation and cautionary remarks

5.1. Some of the short comings of using SR data for obtaining cloud top temperatures are briefly mentioned below keeping in view the operational aspects.

5.1.1. (*i*) Since the resolution of the SR data is about 8 km at best, and is likely to be on the

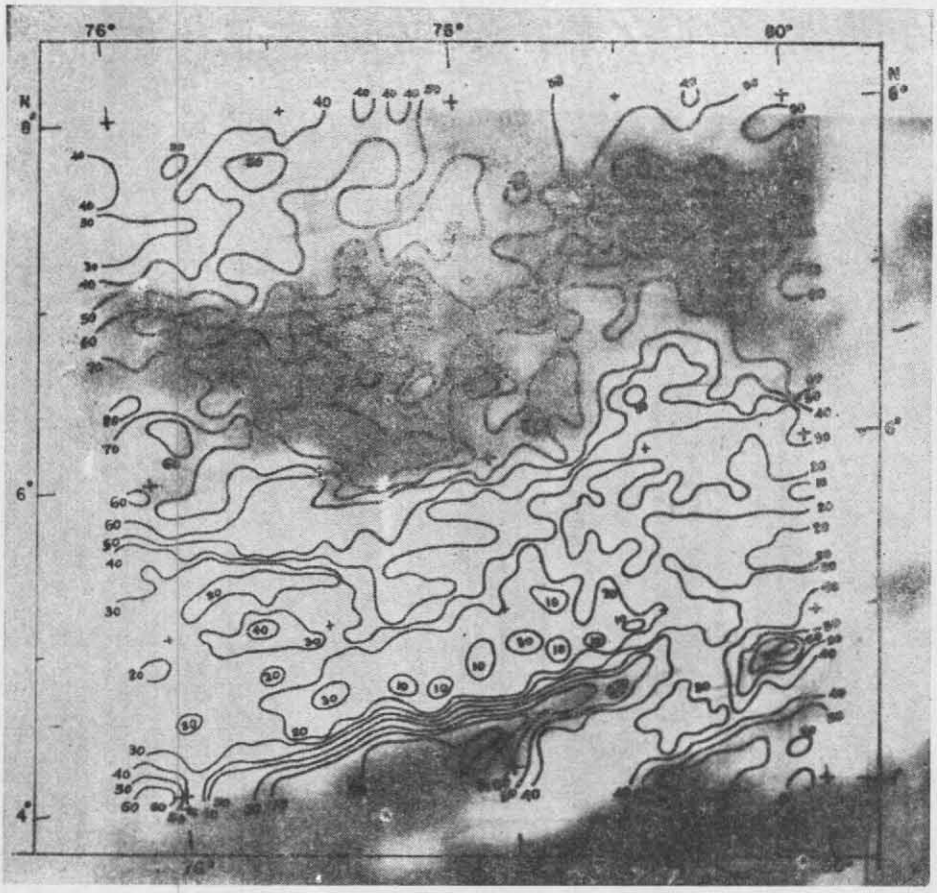

Fig. 13. Isothermal analysis of the temperature field obtained from Nimbus III HRIR data of 1800GMT of 24 Jul 1969

average about 10 to 15 km even in the central portion of the picture, there is an inherent averaging of temperatures within the field in view, with the result that any high *Cb* top whose horizontal dimensions do not exceed 8 km, is likely to be missed or in other words, it is quite possible that the lowest temperatures may not correspond to the maximum height in the case of cellular convective clouds. Further, the truncation of HRIR data at 210°K leaves interminate cloud tops above the level of, say, 14 km or so.

(*ii*) When grid point values are taken, a further scope for missing arises due to the fact that very low temperatures covering small horizontal extent may fall in between two grid points. This also tends to suggest cloud tops at lower heights than are actually present.

(*iii*) It is well realised that thin cirrus overcast cannot be seen in cloud imagerys from satellites. However, they can more or less uniformly lower the temperature values. The estimates of such lowering for *Ci* below the level of discernment is estimated to be about 2 to 5 degrees. While this may not significantly affect the inferences cloud tops, say upto about 12 km in the tropics, can lead to over estimation of clouds above that height due to the fact that the normal lapse rates at high altitudes below the tropopause are usually small.

(*iv*) The short-comings in gridding experienced in this study have already been discussed in section 3·1.

So, in using the SR data for obtaining cloud tops, these limitations need be kept in mind.

6. Discussions of the results and conclusions

(*i*) The analysis in thermal field has shown the three dimensional structure of the cloud fields associated with the two synoptic situations under study. Clouds with estimated heights above 12 km were found on both the occasions, some of the clouds being at heights greater than 14 km. In the case of the cyclonic storm, clouds with maximum heights (greater than 14 km) were found in the central overcast area and the heavily overcast

area to the NE of it and also in the spiral bands. The zonal and meridional cross-sections of cloud heights obtained by using these data show typical characteristics of a storm system even though the storm lies well in land.

(*ii*) The frequency analysis of the equivalent height data has demonstrated the usefulness of the method in drawing conclusions as to the spatial distribution of convective clouds with significant vertical development.

It is to be concluded from the present study that a potentially useful method of evaluating the three dimensional picture of the cloud structures associated with different types of synoptic situations for meeting the day to day operational needs can be developed on real time analysis of High Resolution Infra-Red Scanning Radiometer data, since the above analysis is amenable to computer methods. Such information on cloud tops cannot possibly be obtained by any other method over vast stretches of oceanic areas or even land areas which are not under surveillance of ground based radars equipped with devices or obtaining cloud tops. On the other hand, the demand for such information is already there especially in the case of high-flying aircraft like the present day jets and will continue to increase with the introduction of supersonic aircraft.

Acknowledgements

We wish to thank Shri George Alexander, Deputy Director General of Observatorties for his kind encouragement, in this work. We wish to thank S/Shri P. V. Pathak and S. S. Bhondve for their fine work in preparing the required diagrams and Shri D.V. Vaidya for his general assistance.

REFERENCES

Brawn, Charles 1971 "Limits on accuracy of IR Radiation measurements of sea surface temperature from a satellite" NOAA Tech. Memo. NESS 30

Fujita, T. 1968 "Outflow from a large Tropical cloud Mass" Proc. of the Regional Training Seminar on the Interpretation of Met. Sat. data—Melbourne, 25 Nov-6 Dec 1968, pp, 73, W.M.O.

Hubert, L. F., Timchalk, A. and Fritz, A. 1969 "Estimating maximum wind speed of tropical storms from HRIR Data", NESC Tech. Rep. 50.

Krishna Rao, P. 1970 "Estimating cloud amount and height from Sat. IR data", ESSA Tech. Rep., NESC 54.

Smith, W. L., Rao, P. K., Koffler, R. and Curtis, W. R. 1970 *Mon. Wea. Rev.*, **98**, pp. 604-611.

Srinivasan, V. 1971 *Indian J. Met. Geophys.*, **21**, pp. 643- 646.

Warneck, G., Allison L, and Forshee, L.L. 1967 "Observations of sea surface temperatures and ocean current from Nimbus-II". Space Research VII, pp. 1016-1023. North Holland Publishing Co.